Resonance phenomena and threshold features in positron–helium scattering*

Yu Rong-Mei(于荣梅), Cheng Yong-Jun(程勇军), Wang Yang(王 旸), and Zhou Ya-Jun(周雅君)†

The Academy of Fundamental and Interdisciplinary Sciences, Harbin Institute of Technology, Harbin 150081*, China*

(Received 9 January 2012; revised manuscript received 12 February 2012)

Investigations of resonances and threshold behaviors in positron–helium scattering have been made using the momentum-space coupled-channels optical method. The positronium formation channels are considered via an equivalent-local complex potential. The s-wave resonances and the Wigner cusp feature at the positronium ($n = 1$) formation threshold are compared with the previous reports. The p- and the d-wave resonances and a Wigner cusp feature at the positronium ($n = 2$) formation threshold are reported for the first time.

Keywords: positron, helium, resonance

PACS: 34.80.Uv **DOI:** 10.1088/1674-1056/21/5/053402

1. Introduction

During the past decades, the study of positron-atom and molecule interaction has been an active area of theoretical and experimental research.[1,2] Recently, attention has been drawn to the existence of chemical compounds between antimatter and matter. Predictions of positron bound states with neutral atoms and molecules have important implications for positron and positronium (Ps) chemistry. The bound or quasi-bound (resonance) of positron and Ps to atoms and molecules is a subject of intense studies. Resonance states have been studied extensively in positron–hydrogen[3−8] and positron–alkali-metal[9−16] systems. Positron–helium scattering is the simplest system involving many-body dynamics. The many-body problem brings a challenge to the theoretical treatment. Proper theoretical approaches can reduce the many-body problem to a three-body one. Resonances in the electron–helium system have been the subject of the most extensive theoretical and experimental investigations, in contrast, the theoretical studies for resonances in the positron–helium collision have been very limited so far. Adhikari and Ghosh[17] calculated the total cross sections and predicted an s-wave resonance using the close-coupling approximation with the basis consisting of five helium states and three positronium states. Using the stabilization method, Kar and Ho[18] predicted two s-wave resonances. Very recently, Ultamuratov *et al.*[19,20] reported that there was no resonance in the positron–helium collision using the two-center convergent close-coupling approach. In their calculations, the positronium formation channel was included and multiconfigurational wavefunctions were used to describe the target helium. Subsequently, Ren *et al.*[21] predicted four s-wave resonances in the positron–helium scattering using the same method as that used by Kar and Ho[18] but in the framework of the hyperspherical coordinates. Due to the complexity of the many-body two-center problem, more theoretical and experimental works are needed.

In the present work, the momentum-space coupled-channels optical (CCO) method for the positron–atom scattering[22] is applied to study the energy dependent phenomena in the positron–helium system. The method uses an equivalent-local potential to describe the target continuum and the rearrangement process, and solves the coupled integral equations for discrete channels. The method has been applied to calculate various scattering cross sections (positronium formation, ionization, and total scattering cross sections) for the positron–atom systems, and satisfactory results have been obtained comparing with the experimental data and the other theoretical results.[23−25] Recently, the method has also been applied to investigate the resonance phenomena in positron–atom[14,26] systems. In the present work, s-, p-, and d-wave resonances in the positron–helium system have been determined, and the cusp features at the thresholds of Ps ($n = 1, 2$) have been found. The cusp feature at the Ps ($n = 1$) threshold

*Project supported by the National Natural Science Foundation of China (Grant No. 10674055).

†Corresponding author. E-mail: yajunzhou2003@yahoo.com.cn

© 2012 Chinese Physical Society and IOP Publishing Ltd

found in the present work is consistent with the previous theoretical calculations[27,28] and the experimental measurements.[29] To the best of our knowledge, resonances with angular momentums of $L = 1$ and $L = 2$ and the cusp feature at the Ps ($n = 2$) threshold are reported for the first time.

2. Model and method

The resonance position can be determined by calculating the cross sections of positron scattering. The T-matrix element for the positron–helium collision is calculated by solving coupled integral equations in momentum space[30]

$$\begin{aligned}&\langle \boldsymbol{k}i|T|0\boldsymbol{k}_0\rangle\\ =&\langle \boldsymbol{k}i|V^{(Q)}|0\boldsymbol{k}_0\rangle + \sum_{j\in P}\int \mathrm{d}^3q \frac{\langle \boldsymbol{k}i|V^{(Q)}|j\boldsymbol{q}\rangle\langle \boldsymbol{q}j|T|0\boldsymbol{k}_0\rangle}{E^{(+)} - \epsilon_j - q^2/2},\end{aligned}$$

where i and j represent the target states in P space, and q is an arbitrary momentum of the incident positron. The target ionization continuum and the discrete positronium formation channels are included in the Q space via an optical potential $V^{(Q)}$, which is the channel-coupling potential V plus a complex polarization potential $W^{(Q)}$

$$W^{(Q)} = W_{\mathrm{I}}^{(Q)} + W_{\mathrm{Ps}}^{(Q)}, \tag{1}$$

where $W_{\mathrm{I}}^{(Q)}$ and $W_{\mathrm{Ps}}^{(Q)}$ stand for the parts of the polarization potential that describe the ionization continuum and the positronium formation process, respectively. The form used for the matrix element of polarization potential $W_{\mathrm{I}}^{(Q)}$ was given by McCarthy and Stelbovics.[30]

The matrix element of the optical potential for the positronium formation is

$$\begin{aligned}&\langle \boldsymbol{k}'i|W_{\mathrm{Ps}}^{(Q)}|j\boldsymbol{k}\rangle\\ =&\sum_n \langle \boldsymbol{k}'i|V|\tilde{\chi}_n^{(-)}\rangle \frac{1}{E^{(+)} - \epsilon_n - \frac{1}{4}k_{\mathrm{Ps}}^2}\langle \tilde{\chi}_n^{(-)}|V|j\boldsymbol{k}\rangle,\end{aligned} \tag{2}$$

where $|\chi_n^{(-)}\rangle$ is orthogonalized to the ground state of helium $|\psi_i\rangle$, $|\tilde{\chi}_n^{(-)}\rangle = (1 - |\psi_i\rangle\langle\psi_i|)|\chi_n^{(-)}\rangle$.

The model used for the positronium formation is

$$|\chi_n^{(-)}\rangle = |\phi_\mu \,\mathrm{e}^{\mathrm{i}\,\boldsymbol{k}_{\mathrm{Ps}}\cdot\boldsymbol{R}}\rangle, \tag{3}$$

where ϕ_μ is the bound state of Ps, and $\boldsymbol{k}_{\mathrm{Ps}}$ is the momentum of the Ps center of mass. The plane wave $\mathrm{e}^{\mathrm{i}\,\boldsymbol{k}_{\mathrm{Ps}}\cdot\boldsymbol{R}}$ represents the motion of positronium, since only short-range terms in the positronium-ion potential survive. And $\boldsymbol{R} = (\boldsymbol{r}_{\mathrm{p}} + \boldsymbol{r}_{\mathrm{e}})/2$, where $\boldsymbol{r}_{\mathrm{p}}$ and $\boldsymbol{r}_{\mathrm{e}}$ are the coordinates of the positron and the electron, respectively. For the positron collision with atomic helium, matrix element $\langle \tilde{\chi}_n^{(-)}|V|j\boldsymbol{k}\rangle$ can be calculated as

$$\begin{aligned}\langle \tilde{\chi}_n^{(-)}|V|j\boldsymbol{k}\rangle = &\frac{1}{(2\pi)^3}\iint \mathrm{d}^3r_{\mathrm{p}}\mathrm{d}^3r_{\mathrm{e}}\Big[\phi_\mu^*\,\mathrm{e}^{-\mathrm{i}\,\boldsymbol{k}_{\mathrm{Ps}}\cdot\boldsymbol{R}}\\ &\times\Big(-\frac{1}{r} - V_{1\mathrm{s}}(r_{\mathrm{p}})\Big)\psi_j(\boldsymbol{r}_{\mathrm{e}})\,\mathrm{e}^{\mathrm{i}\,\boldsymbol{k}\cdot\boldsymbol{r}_{\mathrm{p}}}\Big],\end{aligned} \tag{4}$$

where $\psi_j(\boldsymbol{r}_{\mathrm{e}})$ is the bound state of the target atom, $V_{1\mathrm{s}}(r_{\mathrm{p}}) = -\int \mathrm{d}^3r_{\mathrm{e}}\dfrac{|\psi_{1\mathrm{s}}(\boldsymbol{r}_{\mathrm{e}})|^2}{\boldsymbol{r}_{\mathrm{p}} - \boldsymbol{r}_{\mathrm{e}}}$ is the electrostatic potential of the valence electron in the target atom. This potential is expressed as

$$\begin{aligned}V_{1\mathrm{s}}(r_{\mathrm{p}}) = &\sum_{ij} c_{ij}\frac{n_{ij}!}{\xi_{ij}^{n_{ij}+1}}\Big(\frac{\mathrm{e}^{-\xi_{ij}r_{\mathrm{p}}}}{r_{\mathrm{p}}} - \frac{1}{r_{\mathrm{p}}}\Big)\\ &+\sum_{ij} c_{ij}\sum_{k=0}^{n_{ij}-1}\Big[\frac{n_{ij}!}{(n_{ij}-k)!} - \frac{(n_{ij}-1)!}{(n_{ij}-1-k)!}\Big]\\ &\times\frac{1}{\xi_{ij}^{k+1}}r_{\mathrm{p}}^{n_{ij}-1-k}\,\mathrm{e}^{-\xi_{ij}r_{\mathrm{p}}},\end{aligned} \tag{5}$$

where

$$c_{ij} = c_ic_j,\ n_{ij} = n_i + n_j,\ \xi_{ij} = \xi_i + \xi_j, \tag{6}$$

and c, n, and ξ are the parameters of the Slater-type wave function

$$\psi_j = \sum_i c_iA_ir^{n_i-1}\,\mathrm{e}^{-\xi_ir}\mathrm{Y}_{lm}(\boldsymbol{r}). \tag{7}$$

An equivalent-local approximation has been used to the whole polarization potential $W^{(Q)}$ for computational feasibility. The detail of the approximation was given in Ref. [31].

We make a partial-wave expansion of T by defining the partial matrix elements $\langle k'n'l'L' \parallel T_J \parallel Llnk\rangle$ for total orbital angular momentum quantum number J as

$$\begin{aligned}&\langle k', i \mid T \mid j, k\rangle\\ =&\sum_{L,M,L',M',J,K}\langle k' \mid L'M'\rangle\\ &\times C_{L'\ l'}^{M'm'k}\langle k'n'l'L' \parallel T_J \parallel Llnk\rangle C_{LlJ}^{Mmk}\langle LM \mid k\rangle,\end{aligned} \tag{8}$$

where $\langle k \mid LM\rangle \equiv \mathrm{Y}_{LM}(k)$, and C_{LlJ}^{Mmk} is the Clebsch–Gordan coefficient. The definition of $\langle k'n'l'L' \parallel V^Q \parallel Llnk\rangle$ for $V^{(Q)}$ is analogous to Eq. (8) with T_J substituted by V^Q.

The partial-wave cross section from channel j to channel i can be calculated from the partial matrix element

$$\begin{aligned}\sigma_{ij}^{(J)} = &(2\pi)^4\frac{k_i}{k_j}\frac{\widehat{S}^2}{\widehat{l}^2}\frac{1}{4\pi}\\ &\times\sum_{L,L'}(2J+1)|\langle k'n'l'L' \parallel T_J \parallel Llnk\rangle|^2.\end{aligned} \tag{9}$$

The energies and the widths of the resonances for particular values of J have been found by fitting the

Breit–Wigner form with a linear background

$$\sigma_{\rm R}^{(J)} = \left| aE + b + \frac{c + {\rm i}\, d}{E - E_{\rm R} + 0.5\,{\rm i}\,\Gamma_{\rm R}} \right|^2 \qquad (10)$$

to the partial cross section $\sigma_{\rm R}$ for each resonance over the resonance energy range, where E is the incident energy, and $E_{\rm R}$, $\Gamma_{\rm R}$, a, b, c, and d are the fitting parameters. Here $E_{\rm R}$ is the resonant energy, and $\Gamma_{\rm R}$ is the width.

3. Results and discussion

In the present calculation, the P space consists of ten discrete channels. They are 1^1S, 2^1S, 3^1S, 4^1S, 5^1S; 2^1P, 3^1P, 4^1P; 3^1D, 4^1D. The optical potentials describing the target continuum are in the channel couplings 1^1S–1^1S, 1^1S–2^1S, and 1^1S–2^1P. The optical potentials describing the positronium formation in its $n = 1$ and $n = 2$ states are included in the 1^1S–1^1S channel coupling. The optical potentials in the other couplings have a small effect on the cross sections. The target states are represented by configuration-interaction (CI) wave functions. The configuration-interaction calculation of these states is based on ten orbitals, i.e., 1s, 2s, 3s, 4s, 5s; 2p, 3p, 4p; 3d, 4d.

In the present work, we have calculated the total partial wave cross sections from 19.0 eV to 24.1 eV to hunt for resonances. In the present case, only the real part of the potential that represents the polarization of the target is explicitly coupled, since the incident energies are less than the ionization threshold of helium. The s-, p-, and d-wave cross sections in the resonance region for the positron scattering by helium are displayed in Figs. 1–3, respectively.

The s-wave resonance parameters compared with the results of stabilization[18,21] and close-coupling[17] methods are listed in Table 1. The resonance obtained by Ahikari and Ghosh[17] at 19.267 eV is not found in the present calculation. They compared that resonance with a similar s-wave resonance at 19.3 eV[32] in the electron–helium system. In order to check the validity of the present method, we have performed the calculation for the electron–helium scattering from 19.00 eV to 19.50 eV and find the well-established resonance at 19.36 eV but no evidence for the resonance structure occurred over this energy range for the positron–helium scattering. As shown in Fig. 1, a narrow and isolated structure has been found at 20.301 eV with width 0.006 meV below the He(2^1S) threshold. The second s-wave resonance is obtained at 20.661 eV with width 0.5 meV just above the He(2^1S) threshold. We compare these two s-wave resonances with those previously found in the electron–helium system at 20.3 eV[33] and 20.59 eV.[34] Burke *et al.*[35] have pointed out that the polarizability is of fundamental importance and plays an important role in producing the resonances close to the excitation thresholds in the electron–helium system. Ryzhikh and Mitroy[36] have predicted that the positron can be bound to the metastable states of helium due to the strong polarization potential of the excited states of helium. Our results suggest that similar long-range polarization potentials are also responsible for the appearance of the resonances in the positron–helium system. These two s-wave resonances are probably caused by the 2^1S and 2^1P channel mixing, which forms an attractive polarization potential and gives the resonances. The third s-wave resonance located at 22.505 eV is in excellent agreement with the result of Ren *et al.*,[21] except that width we obtained is broader. Kar and Ho[18] and Ren *et al.*[21] have predicted s-wave resonances at 22.788 eV and 22.783 eV, respectively, which are not found in the present calculations. Besides these resonances, Ren *et al.*[21] have also predicted two s-wave resonances at 22.879 eV and 22.858 eV near the Ps ($n = 2$) threshold. In this energy region, we have not found any resonance, however, we find a Wigner cusp at the Ps ($n = 2$) threshold.

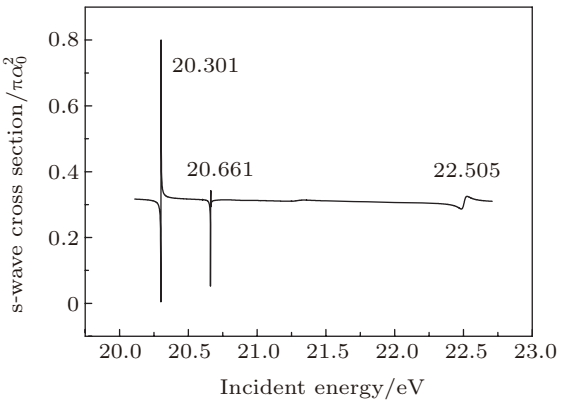


Fig. 1. The s-wave cross sections for positron–helium scattering. Three resonances are predicted to occur at 20.301 eV, 20.661 eV, and 22.505 eV.

Table 1. The s-wave resonances for the positron–helium system. The quoted values for $E_{\rm R}$ are relative to the ground state of helium in the unit of eV. The values in brackets are $\Gamma_{\rm R}$ in the unit of meV.

Present work	Ref. [17]	Ref. [18]	Ref. [21]
	19.267(1)		
20.301(0.006)			
20.661(0.5)			
22.505(39)		22.509(6.9)	22.505(6.3)
		22.788(4.6)	22.783(4.1)
			22.879(1.4)
			22.858(0.5)

The p- and d-wave resonance parameters are listed in Table 2 and displayed in Figs. 2 and 3. No other calculations in the literature are available for

comparison. The lowest-lying p-wave resonance occurs at 20.550 eV below the 2^1S threshold. The second resonance is identified at 20.640 eV lying between the 2^1S and the 2^1P excitation thresholds. We attribute these resonances to the mixing of these two states of helium. We identify three d-wave resonances. Two of them located at 20.790 eV and 21.255 eV are associated with He(1s2s 2^1S) and He(1s2p 2^1P) thresholds, respectively. The third d-wave resonance has been located at 23.472 eV just above the 3^1D and the 3^1P thresholds. We suggest that these three resonance structures are due to the configuration mixing of He(1s3d 3^1D) and He(1s3p 3^1P), which forms the polarization potential and produces these resonances.

Table 2. The p- and d-wave resonances for the positron–helium system. The quoted values for $E_{\rm R}$ are relative to the ground state of helium in the unit of eV. The values in brackets are $\Gamma_{\rm R}$ in the unit of meV.

p-wave	d-wave
20.555(0.005)	20.790(13)
20.640(0.003)	21.255(0.8)
	23.472(38)

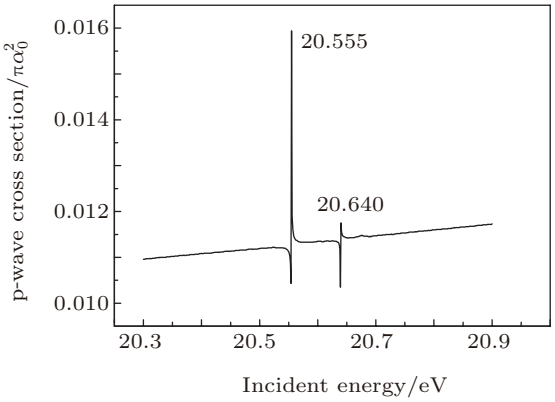


Fig. 2. The p-wave cross sections for positron–helium scattering. Two resonances are predicted to occur at 20.555 eV and 20.640 eV.

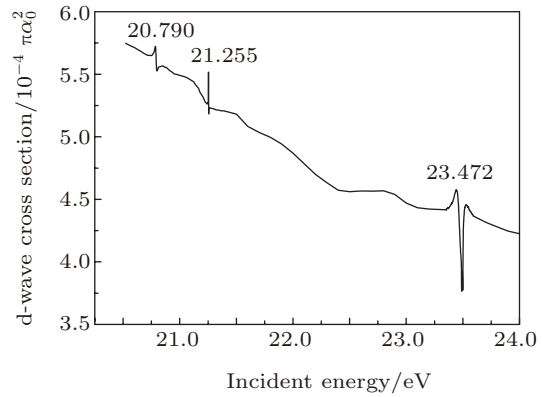


Fig. 3. The d-wave cross sections for positron–helium scattering. Three resonances are predicted to occur at 20.790 eV, 21.255 eV, and 23.472 eV.

In order to exhibit the existence of these resonances, we have plotted the calculation results of the elastic partial wave phase shift as a function of energy in the resonance region in Fig. 4. From the variation of the elastic phase shift, we can find that the phase shift increases by π rad as the energy traverses the resonant energy, which represents a complete description of the resonant behavior.

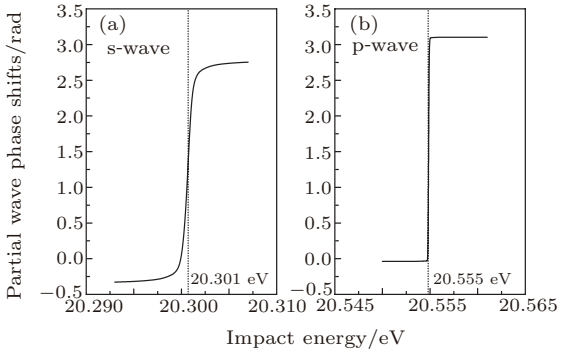


Fig. 4. Partial wave phase shifts near the resonances in the elastic-scattering region for (a) s-wave and (b) p-wave scatterings. The dotted line marks the resonance position where the phase shift is increased by $\pi/2$ rad.

In the present work, we have also investigated the features of the channel-opening threshold. Two Wigner cusps appearing at the positronium formation thresholds are illustrated in Figs. 5 and 6. Threshold effects have been a focus of discussion for many decades since Wigner first predicted the presence of the cusp structures.[37–40] Such a cusp in the electron–helium system has been demonstrated in experimental[41,42] and theoretical[43] works. For the positron–helium scattering, Van Reeth and Humberston[27,28] revealed a significant step-like rise in the total cross section at the Ps ($n = 1$) threshold. Currently, Jones *et al.*[29] have also observed a cusp feature at 17.787 eV in the region of the Ps ($n = 1$) formation threshold. In this paper, we find cusp structures at 17.787 eV in the s-, p-, and d-wave cross sections, as shown in Fig. 5. The present results are consistent with the previous theoretical calculations[27,28] and the experimental measurements.[29] In addition, for the fist time, a small step-like rise that occurs closely to the Ps ($n = 2$) threshold energy 22.887 eV has been found. We identify this structure as a Wigner cusp in the scattering cross section due to the opening of the Ps ($n = 2$) channel. In order to analyze the Wigner cusp features in more detail, we have performed calculations in the CCO+Ps ($n = 1$) model, in which only the Ps ($n = 1$) formation and the continuum part of the optical potential are included in the channel couplings. It is interesting to find that there is no threshold behavior over the Ps ($n = 2$) threshold

region. This indicates that the Wigner cusp at the Ps ($n = 2$) threshold is caused by the opening of the Ps ($n = 2$) formation channel.

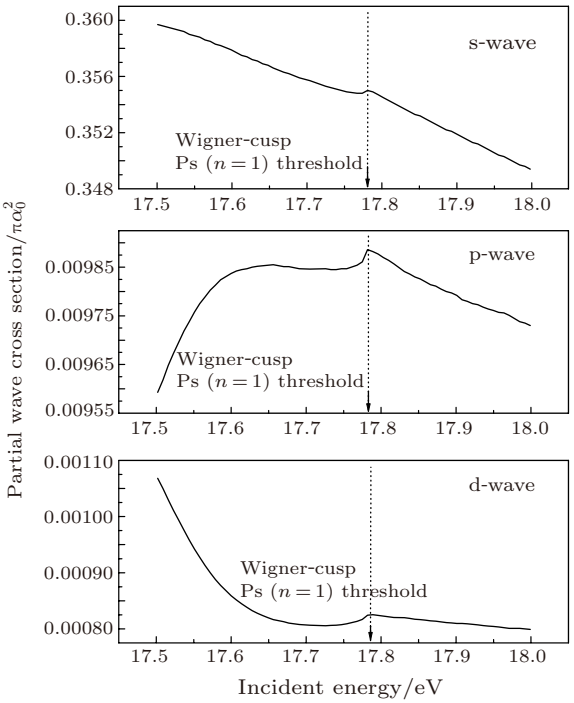


Fig. 5. The Ps ($n = 1$) threshold features in (a) s-, (b) p-, and (c) d-wave cross sections for positron–helium scattering. Arrows mark the centers of the Wigner cusps.

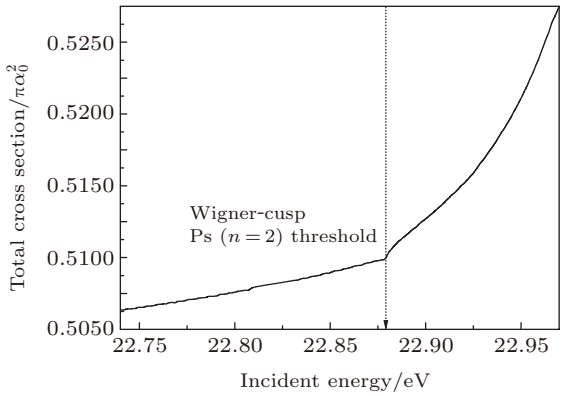


Fig. 6. The Ps ($n = 2$) threshold feature in the total cross sections for positron–helium scattering. The arrow marks the center of the Wigner cusp.

4. Conclusion

In summary, we report a theoretical calculation of s-, p-, and d-wave resonances in positron–helium scattering using the momentum-space coupled-channels optical method. The p- and d-wave resonances are reported for the first time. Our results suggest that the long-range polarization plays an important role in producing the resonances. In the present calculation, we identify a Wigner cusp at the Ps ($n = 1$) threshold, which is consistent with the previous theoretical calculations[27,28] and the experimental measurements.[29] In addition, a cusp feature at the vicinity of the Ps ($n = 2$) threshold is reported for the first time.

References

[1] Xu H X, Hao Y P, Han R D, Weng H M, Du H J and Ye B J 2011 *Acta Phys. Sin.* **60** 067803 (in Chinese)
[2] Qi N, Wang Y W, Wang D, Wang D D and Chen Z Q 2011 *Acta Phys. Sin.* **60** 107805 (in Chinese)
[3] Seiler G J, Oberoi R S and Callaway J 1971 *Phys. Rev.* A **3** 2006
[4] Doolen G D, Nuttall J and Wherry C J 1978 *Phys. Rev. Lett.* **40** 313
[5] Mitroy J and Ratnavelu K 1995 *J. Phys.* B: *At. Mol. Opt. Phys.* **28** 287
[6] Gien T T 1996 *J. Phys.* B: *At. Mol. Opt. Phys.* **29** 2127
[7] Yan Z C and Ho Y K 2008 *Phys. Rev.* A **77** 030701
[8] Ho Y K and Yan Z C 2004 *Phys. Rev.* A **70** 032716
[9] Ward S J, Horbatsch M, McEachran R P and Stauffer A D 1989 *J. Phys.* B: *At. Mol. Opt. Phys.* **22** 3763
[10] McAlinden M T, Kernoghan A A and Walters H R J 1997 *J. Phys.* B: *At. Mol. Opt. Phys.* **30** 1543
[11] Roy U and Ho Y K 2002 *J. Phys.* B: *At. Mol. Opt. Phys.* **35** 2149
[12] Roy U and Ho Y K 2004 *Nucl. Instr. Meth.* B **221** 36
[13] Han H, Zhong Z, Zhang X and Shi T 2008 *Phys. Rev.* A **78** 044701
[14] Liu F, Cheng Y, Zhou Y and Jiao L 2011 *Phys. Rev.* A **83** 032718
[15] Kar S and Ho Y K 2005 *Eur. Phys. J.* D **35** 453
[16] Han H, Zhong Z, Zhang X and Shi T 2008 *Phys. Rev.* A **77** 012721
[17] Ahikari S K and Ghosh A S 1996 *Chem. Phys. Lett.* **262** 460
[18] Kar S and Ho Y K 2004 *J. Phys.* B: *At. Mol. Opt. Phys.* **37** 3177
[19] Utamuratov R, Kadyrov A S, Fursa D V and Bray I 2010 *J. Phys.* B: *At. Mol. Opt. Phys.* **43** 031001
[20] Utamuratov R, Kadyrov A S, Fursa D V and Bray I 2010 *J. Phys.* B: *At. Mol. Opt. Phys.* **43** 125203
[21] Ren Z, Han H and Shi T 2011 *J. Phys.* B: *At. Mol. Opt. Phys.* **44** 065204
[22] Zhou Y, Ratnavelu K and McCarthy I E 2005 *Phys. Rev.* A **71** 042703
[23] Cheng Y J and Zhou Y J 2007 *Phys. Rev.* A **76** 012704
[24] Cheng Y J and Zhou Y J 2010 *Chin. Phys.* B **19** 063405
[25] Cheng Y J, Zhou Y J and Jiao L G 2012 *Chin. Phys.* B **21** 013405
[26] Yu R M, Cheng Y J, Jiao L G and Zhou Y J 2012 *Chin. Phys.* B **21** 013404
[27] Van Reeth P and Humberston J W 1999 *J. Phys.* B: *At. Mol. Opt. Phys.* **32** L103
[28] Van Reeth P and Humberston J W 2000 *Nucl. Instr. Meth.* B **171** 106
[29] Jones A C L, Caradonna P, Makochekanwa C, Slaughter D S, McEachran R P, Machacek J R, Sullivan J P and Buckman S J 2010 *Phys. Rev. Lett.* **105** 073201
[30] McCarthy I E and Stelbovics A T 1983 *Phys. Rev.* A **28** 2693

[31] McCarthy I E and Zhou Y 1994 *Phys. Rev. A* **49** 6
[32] Burke P G, Cooper J W and Ormonde S 1969 *Phys. Rev.* **183** 245
[33] Golden D E and Zecca A 1970 *Phys. Rev.* A **1** 241
[34] Kuyatt C E, Simpson J A and Mielczarek S R 1965 *Phys. Rev.* **138** A385
[35] Burke P G, Cooper J W and Ormonde S 1969 *Phys. Rev.* **183** 345
[36] Ryzhikh G and Mitroy J 1998 *J. Phys.* B: *At. Mol. Opt. Phys.* **31** 3465
[37] Newton R G 1959 *Phys. Rev.* **114** 1611
[38] Meyerhof W E 1963 *Phys. Rev.* **129** 692
[39] Coleman P G, Cheesman N and Lowry E R 2009 *Phys. Rev. Lett.* **102** 173201
[40] Wigner E P 1948 *Phys. Rev.* **73** 1002
[41] Baz A I 1957 *Zh. Eksp. Teor. Fiz.* **33** 923
[42] Sanche L and Schulz G J 1972 *Phys. Rev.* A **5** 1672
[43] Oberoi R S and Nesbet R K 1973 *Phys. Rev.* A **8** 2969